Desalination and Water Treatment
www.deswater.com

10 (2009) 144–147

1944-3994 / 1944-3986

Linearization of ultrafiltration models: analysis of experimental data from ultrafiltration tests

María-Cinta Vincent-Vela[a]*, Silvia Álvarez-Blanco[a], Jaime Lora-García[a], Enrique Bergantiños-Rodríguez[b]

[a]*Department of Chemical and Nuclear Engineering, Polytechnic University of Valencia, C/Camino de Vera s/n 46022 Valencia, Spain Tel. +34 963877000 Ext. 79387; Fax +34 963877639; email: mavinve@iqn.upv.es*
[b]*Department of Chemical Engineering, Polytechnical Institute José A. Echeverría, Ave. 114, No. 11901, Havana, Cuba*

Received 16 July 2008; Accepted in revised form 23 September 2009

ABSTRACT

A great number of models proposed in the literature that describe permeate flux decline with time in ultrafiltration can be linearized to obtain an equation expressed in terms of transmembrane pressure (TMP) divided by permeate flux, $\Delta P^2/J_P^2$, as a function of time. In this work, experimental results from pilot plant ultrafiltration tests are expressed in terms of $\Delta P^2/J_P^2$ vs. time to check their linearity. Regression analysis allowed the determination of the quotient: specific resistance of the gel layer/ gel layer concentration (r_c/C_g). Ultrafiltration tests were performed at constant temperature (25°C) and feed concentration (5 g/L) at different feed flow rates (1–3 m/s) and transmembrane pressures (0.1–0.4 MPa) with monotubular ZrO_2-TiO_2 (molecular weight cut-off: 15 kg/mol) and aqueous solutions of polyethylene glycol (PEG) of 35,000 g/mol.

Keywords: Ultrafiltration; Model; Gel layer resistance; Initial membrane fouling resistance

1. Introduction

There is a great number of models proposed in the literature that attempt to describe membrane ultrafiltration fouling processes [1–9]. Most of them [1–3,6,8,9] can be linearized obtaining an equation expressed in terms of transmembrane pressure (TMP) divided by permeate flux, $\Delta P^2/J_P^2$, as a function of time.

Eqs. (1)–(4) show the linearized forms for: the shear induced diffusion model [10], a model that was developed for dead-end ultrafiltration and afterwards adapted to crossflow UF [10], a model that considers ultrafiltration as a dynamic process that changes from a non-equilibrium condition to an equilibrium condition, where the cake layer thickness remains constant [11] and a model based in the resistance in series model that integrates in the same analytical expression the osmotic pressure as well as gel layer formation [12], respectively.

$$\frac{\Delta P^2}{J_P{}^2} = \left(\mu \cdot R_m\right)^2 + 4 \cdot \frac{\mu^3 \cdot R_m{}^2 \cdot R_c \cdot C_0}{\left(C_g - C_0\right) \cdot \Delta P} \cdot \left(C_{gv} - C_{0v} - C_{0v} \cdot \ln\left(\frac{C_g}{C_0}\right)\right) + 4 \cdot \frac{\mu \cdot R_c \cdot C_0 \cdot \Delta P}{\left(C_g - C_0\right)} t \quad (1)$$

In Eq. (1) J_p is the permeate flux (m s^{-1}), ΔP is the transmembrane pressure (Pa), μ is the dynamic viscosity of the permeate (kg m^{-1}s^{-1}), R_m is the membrane resistance (m^{-1}), R_c is the specific resistance of the gel layer (m^{-2}), C_{0v} is the solute concentration in the feed expressed in volume per volume, C_{gv} is the solute concentration in the gel layer in

* Corresponding author.

Presented at EuroMed 2008, Desalination for Clean Water and Energy Cooperation among Mediterranean Countries of Europe and the MENA Region, 9–13 November 2008, King Hussein Bin Talal Convention Center, Dead Sea, Jordan.

volume per volume, C_0 is the feed concentration (kg m^{-3}), C_g is the gel layer concentration (kg m^{-3}) and t is time (s).

$$\frac{\Delta P^2}{J_P^2} = \left(\mu \cdot R_m\right)^2 + \frac{R_c' \cdot \Delta P \cdot C_0}{C_g - C_0} \cdot t \quad (2)$$

In Eq. (2) R_c' is the specific resistance of the cake layer (m^{-2}).

$$\frac{\Delta P^2}{J_P^2} = \left(\mu \cdot R_m\right)^2 + \frac{2 \cdot r_c \cdot \Delta P \cdot C_0}{C_g} \cdot t \quad (3)$$

In Eq. (3) r_c is the specific resistance of the gel layer (kg m^{-3}s^{-1}).

$$\frac{\Delta P^2}{J_P^2} = \mu^2 \left(R_m + R_a + R_{osm}\right)^2 + 2 \cdot a \cdot \mu \cdot C_0 \cdot t \quad (4)$$

In Eq. (4) R_a is the adsorption resistance (m^{-1}), R_{osm} is the osmotic resistance (m^{-1}) and a is the specific resistance of the gel layer (m kg^{-1}).

In this work, experimental results from ultrafiltration tests are expressed in terms of $\Delta P^2/J_P^2$, as a function of time to check linearity. The parameters R_m and r_c/C_g are determined from the linearized Eq. (3), which corresponds to the one of the most accepted ultrafiltration dynamic models.

2. Materials and methods

Monotubular Carbosep M2 ZrO_2–TiO_2 ceramic membranes supplied by Orelis, S.A. (France) with a molecular weight cut off (MWCO) of 15 KDa were used in the ultrafiltration tests. The membrane area was 35.5 cm^2 and it had an internal diameter of 6 mm.

Polyethylene glycol (PEG) of 35000 g/mol was selected as the feed solute because it has been very often used as a standard macromolecule in fouling ultrafiltration tests carried out for modelling purposes [13,14]. The PEG used in the preparation of the feed aqueous solution was supplied by Merck–Schuchardt (Germany).

The experiments were performed at different feed flow rates (1–3 m/s), transmembrane pressures (TMPs) (0.1–0.4 MPa) and a constant feed concentration (5 g/L). All the experiments were carried out at constant temperature (25°C). Ultrafiltration tests were performed with the ultrafiltration pilot plant described elsewhere [1–3,5,6].

The membrane was cleaned at 40°C with an aqueous NaOH solution of 0.2% w/w in deionised water. The NaOH was supplied by Panreac (Spain). The cleaning protocol managed to recover initial membrane pure water permeability. Consequently, the same membrane was used in all the experiments.

3. Results

Figs. 1–3 illustrate experimental results from ultrafiltration tests expressed in terms of $\Delta P^2/J_P^2$ as a function of time. The symbols correspond to the experimental results and the continuous straight lines to the linear regression of experimental data.

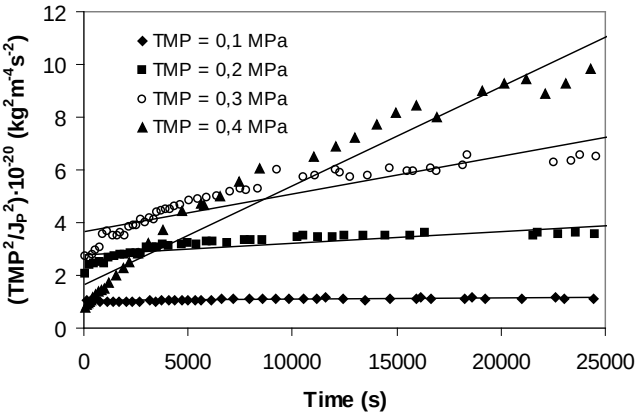

Fig. 1. Experimental data and model predictions for a crossflow velocity of 1 m/s and a feed concentration of 5 g/L.

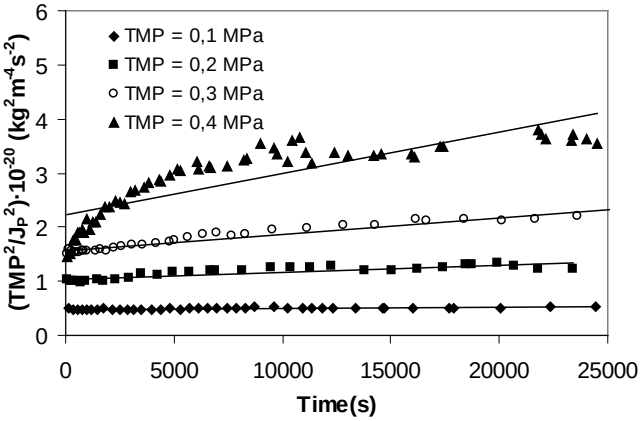

Fig. 2. Experimental data and model predictions for a crossflow velocity of 2 m/s and a feed concentration of 5 g/L.

In Fig. 1 it can be observed that the linearity of the experimental data is the highest for the lowest TMPs tested. For high TMPs experimental data show a linear tendency for time scales larger than 5000 s.

Comparison of Figs. 1–2 shows that linearity increases with the increase in the crossflow velocity. The results in Fig. 2 confirm that a good linearity is obtained for the experimental results that correspond to TMPs of 0.1, 0.2 and 0.3 MPa, whereas for a TMP of 0.4 MPa linearity of experimental data is only achieved for long time scales.

For the highest crossflow velocity tested (Fig. 3), 3 m/s, it is observed a clear linear tendency when the experimental results are plotted in terms of $\Delta P^2/J_p^2$ as a function of time.

The main reason for the non-linearity of experimental

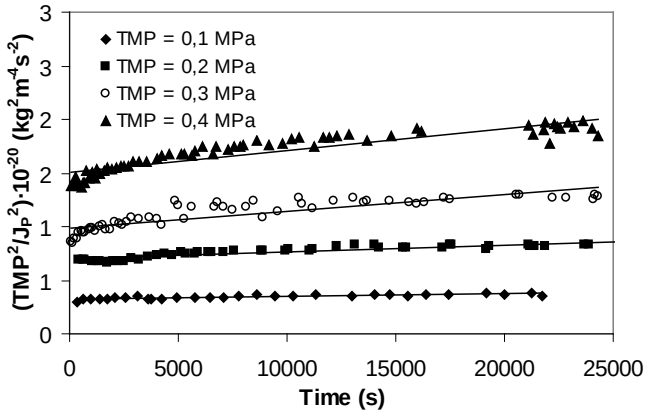

Fig. 3. Experimental data and model predictions for a crossflow velocity of 3 m/s and a feed concentration of 5 g/L.

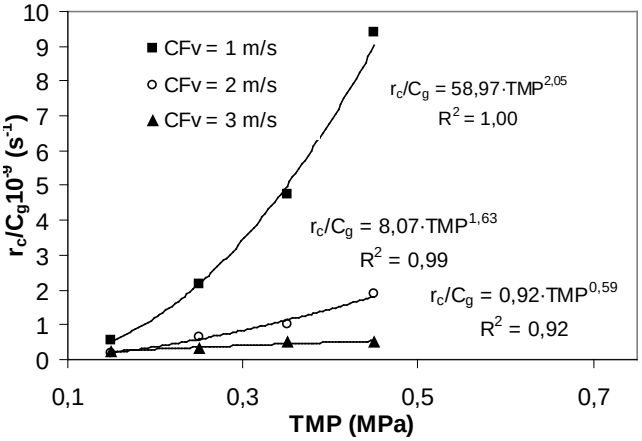

Fig. 4. Variation in the regressed values of r_c/C_g with TMP.

results for all time scales is that several different fouling mechanisms can be occurring at different time scales. Some of them, such as pore blocking, are not considered in the models described here. Pore blocking may occur in the early stages of ultrafiltration. On the other hand this fouling mechanism is more intense at those conditions that cause more severe fouling (i.e. high TMPs and low cross-flow velocities) and linearity was observed to be lower for those operating conditions.

The regression analysis performed in Figs. 1–3 provided a tool to estimate the relation r_c/C_g from Eq. (3). Fig. 4 illustrates the variation in the regressed values of r_c/C_g with TMP. The results show that an increase of TMP and a decease in crossflow velocity resulted in higher values of r_c/C_g. This is consistent with the fact that experimental conditions that favour membrane fouling provide the highest value of fouling resistance. The regression curves together with the values of R^2 are also presented in Fig. 4. The values of R^2 are higher for low crossflow velocities meaning that the best fittings are obtained for the lowest crossflow velocity tested, 1 m/s.

The results presented in Fig. 4 are consistent with the assumption that the variable that controls the values of the quotient r_c/C_g is r_c. For high TMPs and low crossflow velocities the probability of gel layer formation is higher. Consequently, the values of the specific resistance of the gel layer and the values of the gel layer concentration are higher than in the case of low TMPs and high crossflow velocities. The results in Fig. 4 show that the value of the quotient r_c/C_g is the highest for high TMPs and low crossflow velocities.

4. Conclusions

When $\Delta P^2/J_p^2$ is plotted vs. time the linearity of the experimental data obtained in this work is higher for the low TMPs and high crossflow velocities. For high TMPs and low crossflow velocities membrane fouling is higher and several different fouling mechanisms, such as pore blocking in the early stages of ultrafiltration, may be occurring at different time scales. As the models presented in this work do not account for this type of fouling, a linear relationship between $\Delta P^2/J_p^2$ and time is not found for all the experimental conditions tested, particularly at the beginning of ultrafiltration tests.

The results also show that in the case of the experimental conditions for which membrane fouling is more severe, high TMPs and low crossflow velocities, higher values of r_c/C_g are obtained, as expected. These values can be regressed successfully to a power type fitting curve.

Acknowledgements

The authors of this work wish to gratefully acknowledge the financial support of the Spanish Ministry of Science and Technology (MCYT) through the project no. CTQ2005-03398.

References

[1] M.C. Vincent-Vela, S. Álvarez-Blanco, J. Lora-García, J.M. Gozálvez-Zafrilla and E. Bergantiños-Rodríguez, Utilization of a shear induced diffusion model to predict permeate flux in the crossflow ultrafiltration of macromolecules, Desalination, 206 (2007) 61–68.

[2] M.C. Vincent-Vela, S. Álvarez-Blanco and J. Lora-García, Crossflow ultrafiltration of cake forming solutes: a non-steady state model, Desalination, 184 (2005) 347–356.

[3] M.C. Vincent-Vela, S. Álvarez-Blanco, J. Lora-García and E. Bergantiños-Rodríguez, Prediction of flux decline in the ultrafiltration of macromolecules, Desalination, 192 (2006) 323–329.

[4] M.C. Vincent-Vela, S. Álvarez-Blanco, J. Lora-García and E. Bergantiños-Rodríguez, Application of a dynamic model that combines pore blocking and cake formation in crossflow ultrafiltration, Desalination, 200 (2006) 138–139.

[5] M.C. Vincent-Vela, S. Álvarez-Blanco, J. Lora-García and E. Bergantiños-Rodríguez, Application of a dynamic model for predicting flux decline in crossflow ultrafiltration, Desalination. 198 (2006) 303–309.

[6] M.C. Vincent-Vela, S. Álvarez-Blanco, J. Lora-García, J.M. Gozálvez-Zafrilla and E. Bergantiños-Rodríguez, Modelling of flux decline in crossflow ultrafiltration of macromolecules: comparison between predicted and experimental results, Desalination, 204 (2007) 328–334.
[7] M.C. Vincent-Vela, S. Álvarez-Blanco, J. Lora-García and E. Bergantiños-Rodríguez, Fouling dynamics modelling in the ultrafiltration of PEGs, Desalination, 222 (2008) 451–456.
[8] M.C. Vincent-Vela, E. Bergantiños-Rodríguez, S. Álvarez-Blanco and J. Lora-García, Influence of feed concentration on the accuracy of permeate flux decline prediction in ultrafiltration, Desalination, 221 (2008) 383–389.
[9] M.C. Vincent-Vela, S. Álvarez-Blanco, J. Lora-García and E. Bergantiños-Rodríguez, Permeate flux decline prediction in the ultrafiltration of macromolecules with empirical estimation of the gel layer concentration, Desalination, 221 (2008) 390–394.
[10] R.H. Davis, Modeling of fouling of crossflow microfiltration membranes, Separ. Purif. Meth., 21 (1992) 75–126.
[11] L. Song, Flux decline in crossflow microfiltration and ultrafiltration: mechanisms and modeling of membrane fouling, J. Membr. Sci., 139 (1998) 183–200.
[12] S. Bhattacharjee and P.K. Bhattacharya, Flux decline behaviour with low molecular weight solutes during ultrafiltration in an unstirred batch cell, J. Membr. Sci., 72 (1992) 149–161.
[13] S. Ganguly and P.K. Bhattacharya, Development of concentration profile and prediction of flux for ultrafiltration in a radial cross-flow cell, J. Membr. Sci., 97 (1994)185–198.
[14] S. Ghose, C. Battacharjee and S. Datta, Simulation of unstirred batch ultrafiltration process based on a reversible pore-plugging model, J. Membr. Sci., 169 (2000) 29–38.